Available online at www.sciencedirect.com
SCIENCE DIRECT®
Journal of Solid State Chemistry 177 (2004) 38–44
JOURNAL OF SOLID STATE CHEMISTRY
http://elsevier.com/locate/jssc

Studies on magnetic and calorimetric properties of double perovskites Ba_2HoRuO_6 and Ba_2HoIrO_6

Yukio Hinatsu,[a,*] Yuki Izumiyama,[a] Yoshihiro Doi,[a] Abdolali Alemi,[a,1] Makoto Wakeshima,[a] Akio Nakamura,[b] and Yukio Morii[b]

[a] *Division of Chemistry, Graduate School of Science, Hokkaido University, Sapporo 060-0810, Japan*
[b] *Japan Atomic Energy Research Institute, Tokai-mura, Ibaraki 319-1195, Japan*

Received 11 March 2003; received in revised form 6 May 2003; accepted 17 May 2003

Abstract

Magnetic properties of double perovskite compounds Ba_2HoRuO_6 and Ba_2HoIrO_6 have been reported. Powder X-ray and neutron diffraction measurements show that these compounds have a cubic perovskite-type structure with the space group $Fm\bar{3}m$ and the 1:1 ordered arrangement of Ho^{3+} and Ru^{5+} (or Ir^{5+}) over the 6-coordinate *B* sites. Results of the magnetic susceptibility and specific heat measurements show that Ba_2HoRuO_6 exhibits two magnetic anomalies at 22 and 50 K. Analysis of the temperature dependence of magnetic specific heat indicates that the anomaly at 50 K is due to the antiferromagnetic ordering of Ru^{5+} ions and that the anomaly at 22 K is ascribable to the magnetic interaction between Ho^{3+} ions. Neutron diffraction data collected at 10 and 35 K show that the Ba_2HoRuO_6 has a long range antiferromagnetic ordering involving both Ho^{3+} and Ru^{5+} ions. Each of their magnetic moments orders in a Type I arrangement and these magnetic moments are anti-parallel in the *ab*-plane with each other. The magnetic moments are aligned along the *c*-direction. On the other hand, Ba_2HoIrO_6 is paramagnetic down to 1.8 K.

Keywords: Magnetic properties; Specific heat; Perovskite; Magnetic structure; Ruthenium; Holmium; Iridium

1. Introduction

The most stable oxidation state of lanthanide (*Ln*) ions is trivalent, and the electronic configuration of Ln^{3+} ions is [Xe] $4f^n$ ([Xe]: xenon electronic core). Magnetic properties of lanthanide compounds are determined by behavior of the unpaired 4*f* electrons in solids. It is known that they are highly localized electrons and well shielded by the surrounding 5*s* and 5*p* electrons in the outer shell. This makes the magnetic interactions between 4*f* electrons in condensed matter very weak, compared with those between *d* electrons. In fact, many of the lanthanide compounds magnetically order below 4 K [1].

One of the most challenging problems in the modern chemistry of lanthanide compounds is to find a compound in which strong magnetic superexchange interactions between 4*f* electrons exist, which give rise to a long-range magnetic ordering at relatively high temperatures, and to elucidate their mechanism. We have been focusing our attention on the crystal structures of the perovskite-type compounds containing lanthanide ions. The lanthanide ion is relatively large and tends to adopt a high coordination number. Therefore, the lanthanide ion usually sits at the *A* site of the perovskite-oxide ABO_3. Not the *A* site ions but the *B* site ions normally determine the physical properties of the perovskites. The perovskites have the flexibility of chemical composition and the possibility of combination of many kinds of ions. By selecting large alkaline earth elements such as Sr and Ba as the *A* site atoms, one finds that the lanthanides occupy the 6-coordinate *B* sites.

Recently, the solid-state chemistry of mixed-metal oxides containing platinum group metals has attracted a great deal of interest. These materials adopt a diverse range of structures and show a wide range of

*Corresponding author. Fax: 11-746-2557.
E-mail address: hinatsu@sci.hokudai.ac.jp (Y. Hinatsu).
[1] On leave from: Faculty of Chemistry, Tabriz University, Tabriz, Iran.

0022-4596/03/$ - see front matter © 2003 Elsevier Inc. All rights reserved.
doi:10.1016/S0022-4596(03)00302-5

electronic properties. For example, the perovskite $SrRuO_3$ transforms to the ferromagnetic state below 160 K [2] and the layered perovskite Sr_2RuO_4 is a superconductor below 1 K [3]. Many compounds including iridium show magnetic orderings, for example Sr_2IrO_4 and $BaIrO_{3-\delta}$ show a weak ferromagnetic transition at 250 K [4] and a ferromagnetic transition at 180 K [5], respectively. We have been studying the structural chemistry and magnetic properties of double perovskite-type oxides A_2LnMO_6 (A = Sr, Ba; Ln = lanthanide elements; $M = 4d$ or $5d$ transition elements), in which both the Ln and M ions are situated at the B-site of the perovskite ABO_3 and they regularly order [6–12]. These oxides show a variety of magnetic behaviors at low temperatures. We are particularly interested in such compounds containing pentavalent ruthenium or iridium ions. The electronic structures of Ru^{5+} and Ir^{5+} ions are [Kr]$4d^3$ and [Xe]$4f^{14}$ $5d^4$, respectively ([Kr]: krypton electronic core). Such highly oxidized cations from the second or third transition series sometimes show quite unusual magnetic properties.

In this paper, we have studied two compounds Ba_2HoRuO_6 and Ba_2HoIrO_6 in which both the holmium and ruthenium (iridium) ions are accommodated at the B sites of the perovskite ABO_3 and they both contribute to their magnetic properties. Previously, Battle et al. reported that the crystal structure of Ca_2HoRuO_6 was a distorted perovskite with a cation distribution best represented as $Ca_{1.46}Ho_{0.54}[Ca_{0.54}Ho_{0.46}Ru]O_6$ [13]. There is no ordering among the Ca^{2+} or Ho^{3+} ions on either the A or the B sites, but the Ca/Ho ions form a 1:1 ordered arrangement with Ru^{5+} on the B sites. At 4.2 K, the Ru^{5+} ions adopt a Type I antiferromagnetic arrangement but there is no evidence of long range magnetic ordering among the Ho^{3+} ions. For Sr_2HoRuO_6, the magnetic susceptibility and specific heat measurements show the existence of magnetic transition at 36 K [14]. Neutron diffraction data collected at 10 and 25 K indicate that this Sr_2HoRuO_6 exhibits a long range antiferromagnetic ordering involving both Ho^{3+} and Ru^{5+} ions. Each of these ions orders in a Type I arrangement. The field dependence of the magnetization was measured and a small hysteresis loop was found below the magnetic transition temperature, indicating the existence of a weak ferromagnetic moment associated with the antiferromagnetism. For iridium compounds, crystal structures and magnetic properties of a series of A_2LnIrO_6 (A = Sr, Ba) have been reported [7–9,15]. As for Sr_2HoIrO_6 and Ba_2HoIrO_6, they have monoclinic perovskite-type structure with space group $P2_1/n$, and are paramagnetic down to 1.8 K [7,8].

In the case that the barium ion is situated at the A site of the perovskite ABO_3, the deviation from the cubic symmetry of the BO_6 octahedral coordination is expected to be much smaller than the case for A = Sr. In this paper, we will report the crystal and magnetic structures and the magnetic properties of Ba_2HoRuO_6 and Ba_2HoIrO_6 through measurements of their magnetic susceptibility, specific heat and powder neutron diffraction. In addition, we have determined the electronic state of the Ho^{3+} ion in these compounds from the analysis of the temperature dependence of their magnetic entropy data.

2. Experimental

Two polycrystalline samples of Ba_2HoRuO_6 and Ba_2HoIrO_6 were prepared by firing the appropriate amounts of $BaCO_3$, Ho_2O_3 and RuO_2 (or Ir metal powders), first at 900°C for 12 h and then 1200°C for several days in air with several interval grinding and pelleting steps. A diamagnetic Ba_2LuNbO_6 was also prepared. This compound is isomorphous with $Ba_2HoRu(Ir)O_6$ and is needed to estimate the lattice contribution of the specific heat to the total specific heat of $Ba_2HoRu(Ir)O_6$. As starting materials, $BaCO_3$, Lu_2O_3 and Nb_2O_5 were used. The heating procedures were the same as the case for $Ba_2HoRu(Ir)O_6$. The progress of the reactions was monitored by powder X-ray diffraction measurements.

Powder X-ray diffraction measurements were carried out in the region of $10° \leqslant 2\theta \leqslant 120°$ using Cu$K\alpha$ radiation on a Rigaku MultiFlex diffractometer equipped with a curved graphite monochromator.

Powder neutron diffraction profiles for Ba_2HoRuO_6 were measured at 10 K, 35 K, and room temperature using a high-resolution powder diffractometer (HRPD) at the JRR-3M reactor (Japan Atomic Energy Research Institute), with a Ge (331) monochromator ($\lambda = 1.8230$ Å) [16]. Measurements were performed in the range of $10° \leqslant 2\theta \leqslant 120°$. Crystal and magnetic structures were determined by the Rietveld technique, using program RIETAN [17].

The temperature dependence of the magnetic susceptibility was made in an applied field of 0.1 T over the temperature range $1.8\,K \leqslant T \leqslant 300\,K$, using a SQUID magnetometer (Quantum Design, MPMS5S). The susceptibility measurements were performed either using zero field cooling (ZFC) and field cooling (FC) conditions. The former was measured upon heating the sample to 300 K under the applied magnetic field of 0.1 T after zero-field cooling to 1.8 K. The latter was measured upon cooling the sample from 300 to 1.8 K at 0.1 T. The magnetic field dependence of the magnetization was measured in the field range of 0–8.5 T at 1.8, 10, 15, 35, and 60 K.

Specific heat measurements were performed using a relaxation technique by a commercial heat capacity measuring system (Quantum Design, PPMS) in the temperature range 1.8–300 K. The sintered sample in the

form of a pellet was mounted on a thin alumina plate with Apiezon for better thermal contact.

3. Results and discussion

3.1. Crystal structure

The X-ray diffraction data collected on Ba_2HoRuO_6 and Ba_2HoIrO_6 could be indexed in a cubic unit cell with space group $Fm\bar{3}m$. Previously, we reported the crystal structure of Ba_2HoIrO_6 was monoclinic with space group $P2_1/n$ [8] (the lattice parameters were $a = 5.9139(2)$, $b = 5.9048(2)$, $c = 8.3501(3)$, and $\beta = 89.981(8)^\circ$), and this did not agree with the present X-ray and neutron diffraction measurements. This space group $Fm\bar{3}m$ also allows two crystallographically distinct octahedral sites in the double perovskite structure, thus permitting 1:1 ordered arrangement between Ho^{3+} and Ru^{5+} (Ir^{5+}) ions. The deviation from the cubic symmetry of the BO_6 octahedral coordination is not observed. Fig. 1 shows the crystal structure of Ba_2HoRuO_6.

For the diffraction profiles, we have performed the Rietveld analysis. Fig. 2(a) shows the calculated and observed neutron diffraction profiles of Ba_2HoRuO_6 at room temperature. The refined lattice parameters and atomic positions are tabulated in Table 1. The Rietveld analysis for the neutron diffraction profiles of Ba_2HoRuO_6 shows that no oxygen deficiency has been observed, i.e., this compound is oxygen-stoichiometric. The Ru–O bond length (1.954 Å) is almost equal to those in various Ru^{5+} compounds [10–12,18–20] and is shorter than those in Ru^{4+} compounds, for example in $BaRuO_3$ [21]. This result also supports that ruthenium ions in the Ba_2HoRuO_6 are in the pentavalent state. The same result has been observed for the Ir–O bond length (1.97 Å) in the Ba_2HoIrO_6, which indicates that the iridium ions are also in the pentavalent state [7,8,22].

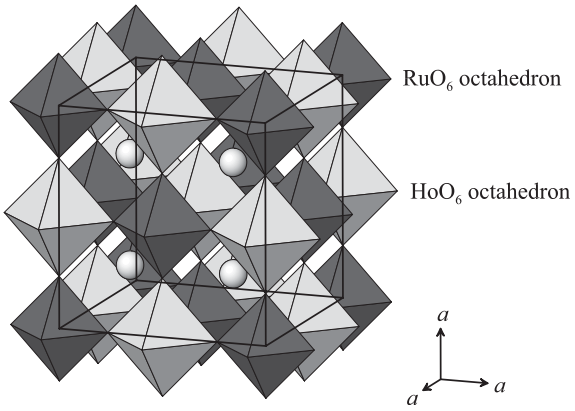

Fig. 1. The crystal structure of Ba_2HoRuO_6. The solid lines indicate the cubic unit cell.

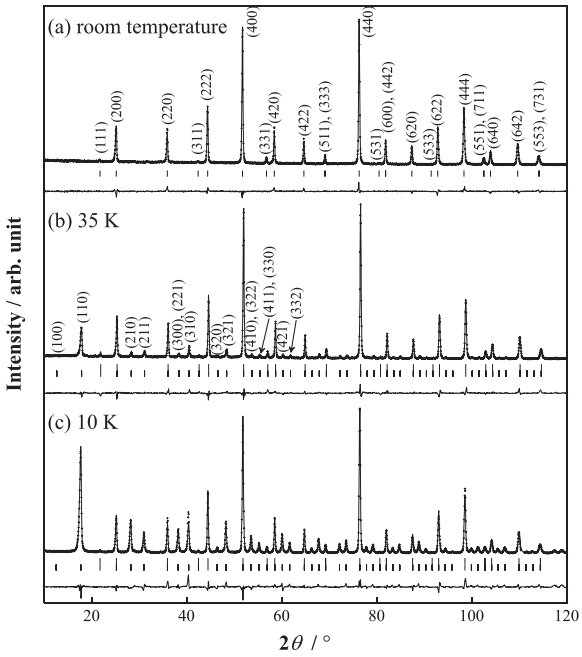

Fig. 2. Powder neutron diffraction profiles for Ba_2HoRuO_6 at (a) room temperature, (b) 35 K, and (c) 10 K. The calculated and observed profiles are shown on the top as solid line and as cross markers, respectively. For (a), the vertical marks in the middle show positions calculated for Bragg reflections. For (b) and (c), the nuclear reflection positions are shown as upper vertical marks and magnetic ones are shown as lower ones. The lower trace is a plot of the difference between calculated and observed intensities.

3.2. Magnetic properties

3.2.1. Ba_2HoRuO_6

The temperature dependence of the magnetic susceptibilities for Ba_2HoRuO_6 is shown in Fig. 3. Two magnetic anomalies have been found at 22 and 50 K. The small magnetic anomaly observed at 50 K is not clear in the magnetic susceptibility vs. temperature curve, the reason for which will be described later. Very small divergence between the ZFC and FC magnetic susceptibilities has been observed below 50 K. The increase of magnetic susceptibility with decreasing temperature below 10 K may be due to a small amount of paramagnetic impurity which was not detected by the diffraction measurements. In the paramagnetic region ($T > 60$ K), the temperature dependence of magnetic susceptibilities follows the Curie–Weiss law and it gives the effective magnetic moment (μ_{eff}) and Weiss constant (θ) to be 10.77(2) μ_B and −19.9(3) K, respectively. Since the theoretical effective magnetic moments of Ru^{5+} and Ho^{3+} (free ion) are 3.87 and 10.58 μ_B, respectively, the expected effective magnetic moment ($\sim 11.27\,\mu_B$) for Ba_2HoRuO_6 is estimated from the relation $\mu_{eff} = \sqrt{\mu^2_{Ru^{5+}} + \mu^2_{Ho^{3+}}}$ The value obtained from the experiment is lower than the calculated value. This result may

Table 1
Structural parameters for Ba_2HoRuO_6

Atom	Site	x	y	z	B (Å^2)	m (μ_B)
At room temperature						
Space group $Fm\bar{3}m$[a]						
Ba	8*c*	1/4	1/4	1/4	0.43(20)	
Ho	4*b*	1/2	1/2	1/2	0.10(13)	
Ru	4*a*	0	0	0	0.36(12)	
O	24*e*	0.2344(9)	0	0	0.73(15)	
$a = 8.3419(1)$ Å, $V = 580.49(1)$ Å^3						
$R_{wp} = 6.73\%$, $R_I = 3.48\%$						
At 35 K						
Space group $Fm\bar{3}m$[a]						
Ba	8*c*	1/4	1/4	1/4	0.37(6)	
Ho	4*b*	1/2	1/2	1/2	0.52(7)	3.84(5)
Ru	4*a*	0	0	0	0.38(5)	2.29(7)
O	24*e*	0.2351(2)	0	0	0.79(5)	
$a = 8.3278(4)$ Å, $V = 578.75(4)$ Å^3						
$R_{wp} = 8.79\%$, $R_I = 4.73\%$, $R_I(\text{mag}) = 6.81\%$						
At 10 K						
Space group $Fm\bar{3}m$[a]						
Ba	8*c*	1/4	1/4	1/4	0.39(7)	
Ho	4*b*	1/4	1/2	1/2	0.20(3)	9.41(6)
Ru	4*a*	0	0	0	0.35(5)	2.79(6)
O	24*e*	0.2351(2)	0	0	0.78(4)	
$a = 8.3139(2)$ Å, $V = 574.67(2)$ Å^3						
$R_{wp} = 10.92\%$, $R_I = 4.49\%$, $R_I(\text{mag}) = 4.37\%$						

Note: Definition of reliability factors R_{wp} and R_I are given as follows. $R_{wp} = [\sum w(|F(o)| - |F(c)|)^2 / \sum w|F(o)^2]^{1/2}$, $R_I = \sum |I_k(o) - I_k(c)| / \sum I_k(o)$.

[a] Space group $Fm\bar{3}m$ applies to the crystal structure.

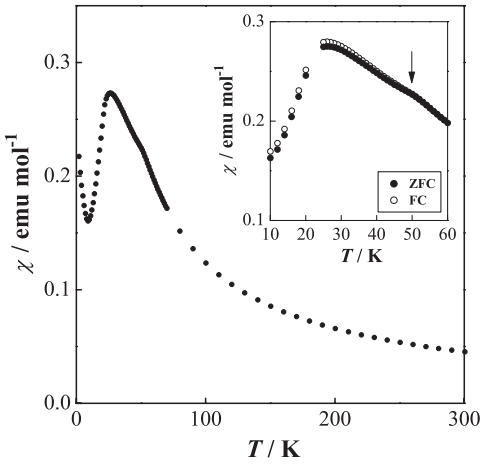

Fig. 3. Temperature dependence of the magnetic susceptibilities for Ba_2HoRuO_6. The inset shows the detailed susceptibility vs temperature curve in the temperature range 10–60 K, and a vertical arrow indicates the temperature at which the ZFC and FC susceptibilities are diverse (see text).

suggest that the magnetic ions in this compound are affected by the crystal field to some extent. The negative Weiss constant indicates that the predominant magnetic interaction in Ba_2HoRuO_6 is antiferromagnetic.

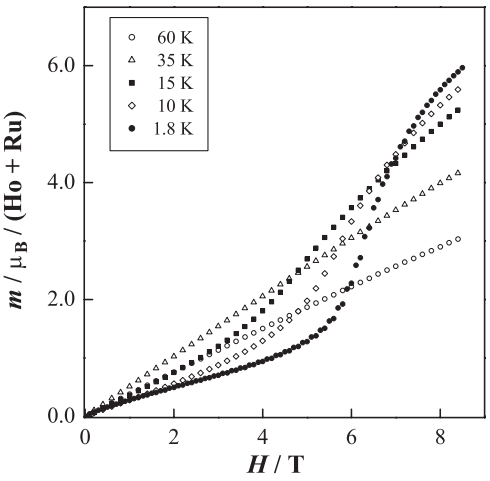

Fig. 4. Field dependence of the magnetization for Ba_2HoRuO_6 at various temperatures.

Fig. 4 shows the field dependence of the magnetization in the range of 0–8.5 T at various temperatures. The magnetic behavior which may be ascribable to the spin–flop transition has been observed at 1.8, 10, and 15 K. If one applies the magnetic field up to 8 T, the saturation of the magnetization will not be observed even at 1.8 K, and the magnetization amounts to 6 μ_B.

Fig. 5 shows the variation of the specific heat for Ba_2HoRuO_6 as a function of temperature. The results of the specific heat measurements are consistent with those by the magnetic susceptibility measurements (Fig. 3), i.e., two λ-type specific heat anomalies have been observed at 22 and 50 K.

In the next step, we will evaluate the magnetic entropy change associated with these antiferromagnetic transitions observed from the magnetic susceptibility and specific heat measurements. In order to know the contribution of the lattice specific heat to the total specific heat for Ba_2HoRuO_6, we used the specific heat data for nonmagnetic Ba_2LuNbO_6 (which is isomorphous with Ba_2HoRuO_6), and its specific heat vs temperature curve is shown in Fig. 5. If we assume that the lattice contribution to the specific heat is equal between Ba_2HoRuO_6 and Ba_2LuNbO_6, the magnetic specific heat (C_{mag}) for Ba_2HoRuO_6 is obtained by subtracting the specific heat of Ba_2LuNbO_6 from that of Ba_2HoRuO_6. The temperature dependence of the magnetic specific heat (C_{mag}) and the magnetic entropy ($S_{mag} = \int (C_{mag}/T)\, dT$) is shown in Fig. 6. Present measurements of the temperature dependence of the magnetic susceptibility and specific heat indicate that there exist two magnetic transitions. We consider that the transition observed at 22 K is due to the magnetic interaction between Ho^{3+} ions and the transition observed at 50 K is ascribable to the antiferromagnetic ordering of Ru^{5+} ions. The reason why the magnetic transition at 50 K is not clear in the

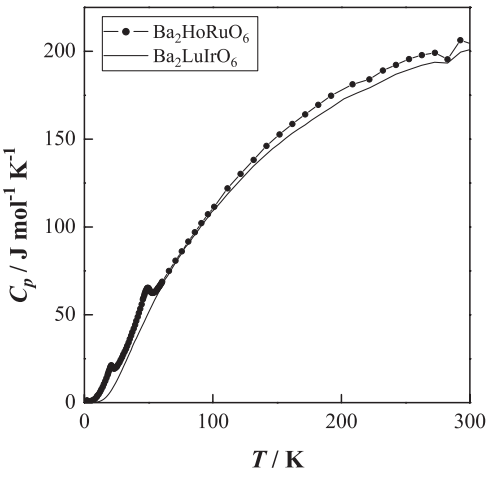

Fig. 5. Temperature dependence of the specific heat for Ba_2HoRuO_6. A solid line represents the specific heat for Ba_2LuNbO_6 (see text).

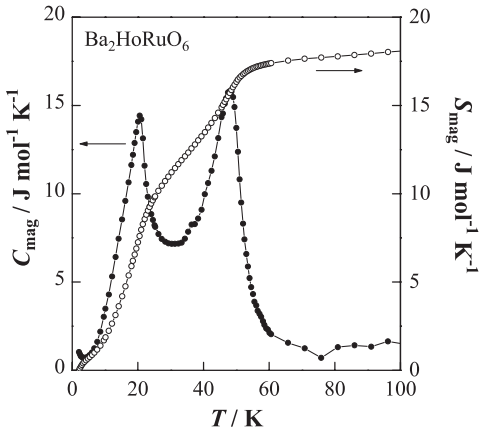

Fig. 6. The magnetic specific heat (C_{mag}) and magnetic entropy (S_{mag}) against temperature for Ba_2HoRuO_6.

magnetic susceptibility vs. temperature curve is due to the smaller magnetic moment of the Ru^{5+} ion ($3.87\,\mu_B$) compared with that of the Ho^{3+} ion ($10.58\,\mu_B$). That is, the paramagnetic behavior of Ho^{3+} ion obscures the antiferromagnetic interaction between the Ru^{5+} ions in the magnetic susceptibility vs. temperature curve.

To estimate the magnetic entropy change due to only the magnetic ordering of Ru^{5+} ions, we evaluated it from the specific heat measurements on Ba_2LnRuO_6 ($Ln = Y$, Lu) in which only the Ru^{5+} ions are paramagnetic. Both the compounds show an antiferromagnetic transition at 37 K which is due to the magnetic interactions between Ru^{5+} ions [18,19], and we have published their results [14]. The magnetic entropy obtained experimentally was $3.9\,J\,mol^{-1}\,K^{-1}$, which is close to $R\ln(2S+1) = R\ln(2\times 1/2+1) = 5.76\,J\,mol^{-1}\,K^{-1}$, meaning that the ground state of the Ru^{5+} ion should be a doublet. That is, although a total spin quantum number of the Ru^{5+} ion is calculated to be $S = 3/2$, the four degenerating states split into two doublets $|S = 3/2,\ M_S = \pm 3/2\rangle$ and $|S = 3/2,\ M_S = \pm 1/2\rangle$ [23]. The magnetic entropy change in the temperature range between 30 and 50 K is close to $R\ln 2$, which indicates that the antiferromagnetic transition at 50 K is due to the antiferromagnetic interaction between Ru^{5+} ions. The magnetic entropy change in the temperature range below 30 K is close to $12\,J\,mol^{-1}\,K^{-1} \sim R\ln 5$ ($J\,mol^{-1}\,K^{-1}$). This result indicates that the degeneracy of the ground state of Ho^{3+} ion should be five, because the magnetic entropy is given by $R\ln W$ (W: degeneracy). In the Ba_2HoRuO_6, the Ho^{3+} ions are surrounded by six oxygen ions. Then, the ground state multiplet $^5I_8$ of the Ho^{3+} ion splits in the octahedral crystalline electric field, and the ground state is a Γ_3 doublet with low-lying excited state (Γ_4 triplet) [24]. The results of the specific heat measurements indicate that their energy separation is very small in this case.

3.2.2. Ba_2HoIrO_6

Fig. 7 shows the temperature dependences of the reciprocal magnetic susceptibility and the specific heat for Ba_2HoIrO_6 in the temperature range of 1.8–300 K. The results of the magnetic susceptibility measurements indicate that this compound is paramagnetic down to 1.8 K. The temperature dependence of magnetic susceptibility follows the Curie–Weiss law and it gives $\mu_{eff} = 10.10(2)\,\mu_B$ and $\theta = -1.9(3)$ K. This value of the effective magnetic moment for Ba_2HoIrO_6 is close to the theoretical effective magnetic moments of Ho^{3+} ion ($10.58\,\mu_B$), which indicates that the magnetic properties of Ba_2HoIrO_6 are mainly determined by the behavior of Ho^{3+} ion. The same results have been observed for other Ba_2LnIrO_6 compounds [8,15]. In addition, we consider the reason why no magnetic ordering has been observed for Ba_2HoIrO_6 in the following. In a strong octahedral crystal field environment, the Ir^{5+} ion has a low spin configuration ($t_{2g}^4 e_g^0 : 5d^4$). In such a case, the effective magnetic moment for Ir^{5+}, μ_{eff} (Ir^{5+}), depends on the ratio of the spin–orbit coupling constant (ζ) to thermal temperature (kT) [25]. When $kT \ll \zeta$, $\mu_{eff}{}^2(Ir^{5+})$ is approximately proportional to temperature T, and therefore the magnetic susceptibility χ (Ir^{5+}) is independent of T [22,26]. Consequently, Ir^{5+} ions no longer contribute to the magnetic cooperative phenomena of perovskite ABO_3, i.e., the occupation of half the B-sites by Ir^{5+} ions causes the magnetic interaction between Ho^{3+} ions to be very weak. Similar results have been observed elsewhere [7,8,15].

The specific heat measurements show that Ba_2HoIrO_6 is paramagnetic down to 10 K, and that there exists a specific heat anomaly at 2.5 K. We believe that this Schottky-type anomaly is due to the crystal field splitting of Ho^{3+} ion [27]. In a similar way as the case for Ba_2HoRuO_6, the contribution of this Schottky-type

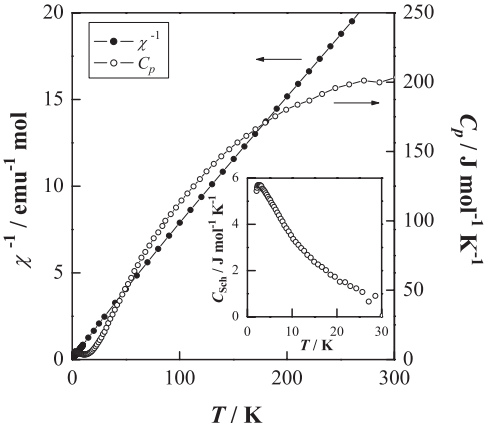

Fig. 7. Temperature dependence of the reciprocal magnetic susceptibility and the specific heat for Ba_2HoIrO_6. The inset shows the detailed Schottky-type specific heat vs temperature below 30 K.

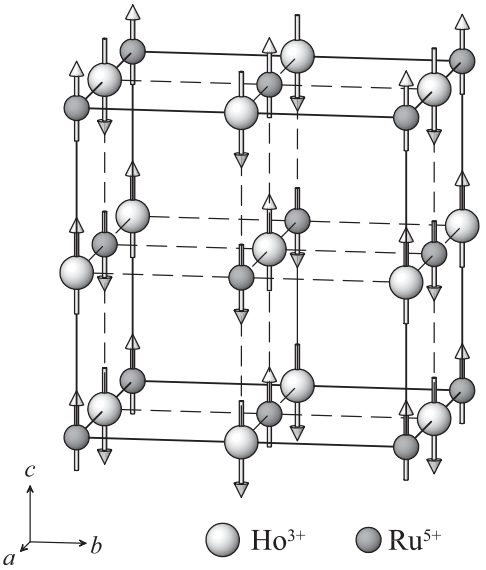

Fig. 8. The magnetic structure of Ba_2HoRuO_6. Diamagnetic ions are omitted. Larger circles, Ho^{3+}; smaller circles, Ru^{5+}. Arrows show the direction of the magnetic moments.

anomaly to the total specific heat is obtained by subtracting the specific heat of Ba_2LuNbO_6 from that of Ba_2HoIrO_6. The residual specific heat is shown in the inset of Fig. 7. On integrating this specific heat, it amounts to $\sim R \ln 5$ (J mol^{-1} K^{-1}). This result indicates that that the Schottky-type anomaly observed at 2.5 K is due to the crystal field splitting of Ho^{3+} ion, in analogy with the case for Ba_2HoRuO_6.

3.3. Magnetic structure of Ba_2HoRuO_6

Since the magnetic anomalies have been observed at 22 and 50 K, powder neutron diffraction measurements have been performed at 10, 35 K, and room temperature, and the diffraction profiles are depicted in Fig. 2. A number of low-angle peaks which were not observed at room temperature appear at 10 and 35 K, indicating that Ba_2HoRuO_6 exhibits long-range magnetic ordering at these temperatures. At low temperatures, there is no difference between the diffraction profiles measured at 10 and 35 K except for their diffraction strengths. These results indicate that both the magnetic moments of Ho^{3+} and Ru^{5+} ions begin to order antiferromagnetically below 50 K. At low temperatures, this Ba_2HoRuO_6 has the same crystal structure as that at room temperature. In the analysis of the neutron diffraction data measured at 10 and 35 K, we assumed that all the magnetic moments were collinear since no magnetic satellite reflections exist. In addition, the size of the magnetic unit cell is the same to that of the crystal unit cell, because there appeared no superlattice reflections. Thus the magnetic unit cell is described as $2a_p \times 2a_p \times 2a_p$, where a_p means a lattice parameter in a primitive cubic perovskite unit cell. In this unit cell, the Ho^{3+} and Ru^{5+} ions form two interpenetrating face-centered sublattices. The main magnetic reflections (100), (010), and (001) determine the direction of the magnetic moments. Then, we have performed the Rietveld analysis and succeeded in determining the magnetic structure, which is illustrated in Fig. 8. In this magnetic structure, each of magnetic moments of Ho^{3+} and Ru^{5+} orders in a type I arrangement. The magnetic moments of the Ho^{3+} and Ru^{5+} ions which exist on the *ab* planes are ordered antiferromagnetically, and the *ab* planes would be ferrimagnetic planes. After all, Ba_2HoRuO_6 is an antiferromagnet in which the ferrimagnetic *ab* planes are stacked antiferromagnetically along the *c*-axis. This magnetic structure has been often found in those for Sr_2LnRuO_6 with $Ln = Tb$ [28], Ho [10], Tm [29] and for Ba_2LnRuO_6 with $Ln = Tm$ [29], and the magnetic moments are aligned along the *c*-direction. The ordered magnetic moments are determined to be 3.84(5) μ_B for Ho^{3+} and 2.29(7) μ_B for Ru^{5+} at 35 K, and 9.41(6) μ_B for Ho^{3+} and 2.79(6) μ_B for Ru^{5+} at 10 K. Since the theoretical value of the ordered magnetic moment for the Ru^{5+} ion which has a d^3 electronic configuration is 3.0 μ_B, it can be said that the magnetic moment of the Ru^{5+} ion in Ba_2HoRuO_6 is almost saturated at 10 K. The results of the magnetic susceptibility, specific heat and magnetic entropy measurements for Ba_2HoRuO_6 show that the magnetic order of the Ru^{5+} ions occur at 50 K, and accordingly it is valid that the ordered magnetic moments of the Ru^{5+} ions are almost saturated at 10 K. On the other hand, the theoretical value of the magnetic moment for the Ho^{3+} ion is $g_J J = 10\,\mu_B$. The magnetic moment of the Ho^{3+} ion is approximately half the theoretical value for the free Ho^{3+} ion at 35 K, and it becomes large at 10 K (9.41(6) μ_B). The variation of the ordered Ho^{3+} moment with temperature means that the magnetic moments of Ho^{3+} ions begin to order with the ordering of the Ru^{5+}

moments at 50 K and they are almost completely ordered at 22 K.

Acknowledgments

The authors are indebted to the Iketani Science and Technology Foundation for the financial support.

References

[1] H.P.J. Wijn, Binary lanthanide oxides, in: Landolt-Bornstein, New Series, Vol. III/4a, Springer, Berlin, 1970.
[2] A. Callaghan, C.W. Moeller, R. Ward, Inorg. Chem. 5 (1966) 1572–1576.
[3] Y. Maeno, H. Hashimoto, K. Yoshida, S. Nishizaki, T. Fujita, J.G. Bednorz, F. Lichtenberg, Nature 372 (1994) 532–534.
[4] M.K. Crawford, M.A. Subramanian, R.L. Harlow, J.A. Fernandez-Baca, Z.R. Wang, D.C. Johnston, Phys. Rev. B 49 (1994) 9198.
[5] A.V. Powell, P.D. Battle, J. Alloys, Compounds 191 (1993) 313.
[6] Y. Doi, Y. Hinatsu, J. Phys.: Condens. Matter 11 (1999) 4813–4820.
[7] D. Harada, M. Wakeshima, Y. Hinatsu, J. Solid State Chem. 145 (1999) 356–360.
[8] M. Wakeshima, D. Harada, Y. Hinatsu, J. Mater. Chem. 10 (2000) 419–422.
[9] D. Harada, M. Wakeshima, Y. Hinatsu, K. Ohoyama, Y. Yamaguchi, J. Phys.: Condens. Matter 12 (2000) 3229–3239.
[10] Y. Doi, Y. Hinatsu, K. Oikawa, Y. Shimojo, Y. Morii, J. Mater. Chem. 10 (2000) 797–800.
[11] Y. Izumiyama, Y. Doi, M. Wakeshima, Y. Hinatsu, K. Oikawa, Y. Shimojo, Y. Morii, J. Mater. Chem. 10 (2000) 2364–2367.
[12] Y. Izumiyama, Y. Doi, M. Wakeshima, Y. Hinatsu, K. Oikawa, Y. Shimojo, Y. Morii, J. Phys.: Condens. Matter 13 (2001) 1303–1313.
[13] P.D. Battle, C.W. Jones, F. Studer, J. Solid State Chem. 90 (1991) 302–312.
[14] Y. Izumiyama, Y. Doi, M. Wakeshima, Y. Hinatsu, A. Nakamura, Y. Morii, J. Solid State Chem. 169 (2002) 125–130.
[15] M. Wakeshima, D. Harada, Y. Hinatsu, N. Masaki, J. Solid State Chem. 147 (1999) 618–623.
[16] Y. Morii, J. Cryst. Soc. Jpn. 34 (1992) 62.
[17] F. Izumi, in: R.A. Young (Ed.), The Rietveld Method, Oxford University Press, Oxford, 1993 (Chapter 13).
[18] P.D. Battle, J.B. Goodenough, R. Price, J. Solid State Chem. 46 (1983) 234–244.
[19] P.D. Battle, W.J. Macklin, J. Solid State Chem. 54 (1984) 245–250.
[20] P.D. Battle, C.W. Jones, J. Solid State Chem. 78 (1989) 108–116.
[21] A. Santoro, I. Natali Sora, Q. Huang, J. Solid State Chem. 151 (2000) 245–252.
[22] M. Wakeshima, D. Harada, Y. Hinatsu, J. Alloys Compd. 287 (1999) 130–136.
[23] D. Harada, Y. Hinatsu, J. Solid State Chem. 158 (2001) 245–253.
[24] K.R. Lea, M.J.M. Leask, W.P. Wolf, J. Phys. Chem. Solids 23 (1962) 1381.
[25] M. Kotani, J. Phys. Soc. Jpn. 4 (1949) 293.
[26] H. Nishimine, M. Wakeshima, Y. Hinatsu, J. Solid State Chem., submitted for publication.
[27] R.L. Carlin, Magnetochemistry, Springer, Berlin, 1986, p. 45.
[28] Y. Doi, Y. Hinatsu, K. Oikawa, Y. Shimojo, Y. Morii, J. Mater. Chem. 10 (2000) 1731–1735.
[29] Y. Doi, Y. Hinatsu, A. Nakamura, Y. Ishii, Y. Morii, J. Mater. Chem. 13 (2003) 1758–1763.